

1 **Dynamic marine viral infections and major contribution to photosynthetic processes shown**
2 **by regional and seasonal picoplankton metatranscriptomes**

3
4 Sieradzki Ella T.¹, Ignacio-Espinoza J. Cesar¹, Needham David M.², Fichot Erin B.¹ and
5 Fuhrman Jed A.^{1,*}

6
7 Author affiliations: (1) University of Southern California, (2) Monterey Bay Aquarium Research
8 Institute

9 * Corresponding author

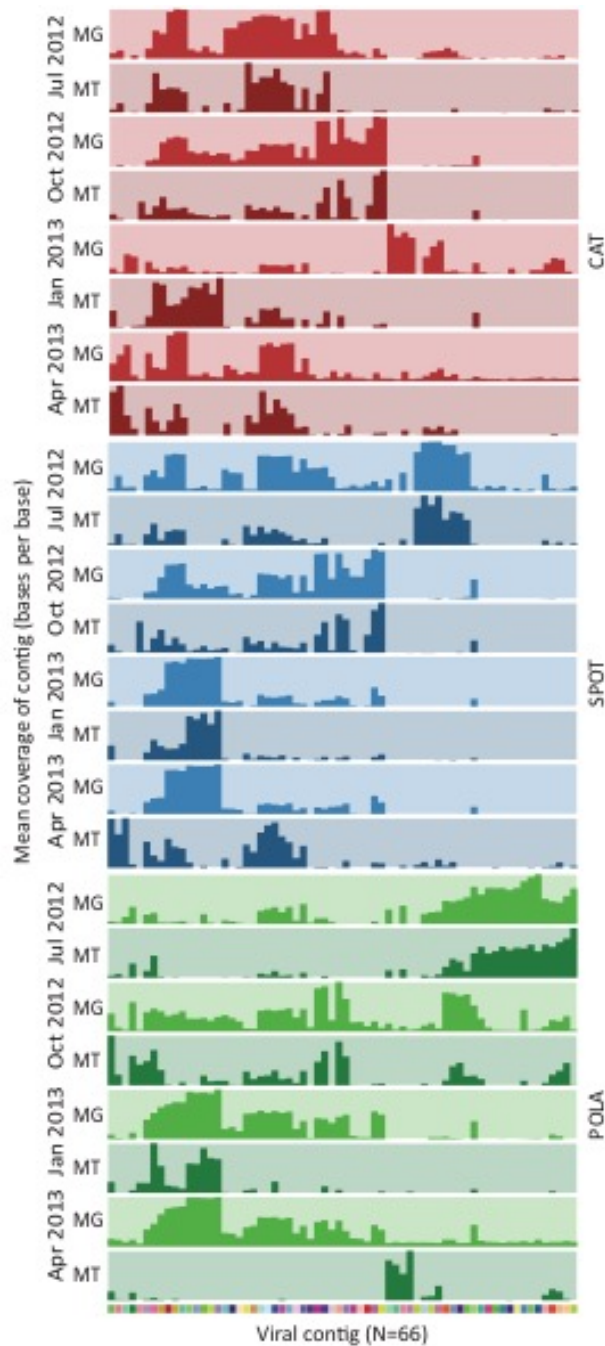
10

11 **Viruses are an important top-down control on microbial communities, yet their direct**
12 **study in natural environments has been hindered by culture limitations¹⁻³. The advance of**
13 **sequencing and bioinformatics over the last decade enabled the cultivation independent**
14 **study of viruses. Many studies focus on assembling new viral genomes⁴⁻⁶ and studying viral**
15 **diversity using marker genes amplified from free viruses^{7,8}. We used cellular**
16 **metatranscriptomics to study community-wide viral infections at three coastal California**
17 **sites throughout a year. Generation of and recruitment to viral contigs (> 5kbp, N=66)**
18 **allowed tracking of infection dynamics over time and space. Here we show that while these**
19 **assemblies represent viral populations, they are likely biased towards clonal or low**
20 **diversity assemblages. Furthermore, we demonstrate that published T4-like cyanophages**
21 **(N=50) and pelagiphages (N=4), having genomic continuity between close relatives, are**
22 **better tracked using marker genes. Additionally, we demonstrate determination of**
23 **potential hosts by matching infection dynamics with microbial community composition.**
24 **Finally, we quantify the relative contribution of various cyanobacteria and viruses to**
25 **photosystem-II *psbA* expression in our study sites. We show sometimes >50% of all**
26 **cyanobacterial+viral *psbA* expression we observed is of viral origin, which highlights the**
27 **proportion of infected cells and makes viruses a remarkable contributor to photosynthesis**
28 **and oxygen production.**

29

30 We sampled surface seawater in different seasons over three sites across the San Pedro Channel,
31 California, USA: The Port of Los Angeles (POLA), Santa Catalina Island Two Harbors (CAT)
32 and the San Pedro Ocean Time-series (SPOT). These sites represent a gradient of human impact
33 with POLA being the most impacted and SPOT resembling open ocean conditions. In all of these
34 sites free virus-like particles outnumber bacteria and archaea roughly 10:1 (sup. fig. 1). We
35 examined only the 0.2-1 μm size-fraction, which includes most bacteria, archaea and some
36 picoeukaryotes. Via assembly of metatranscriptomes, we obtained 1455 contigs longer than 5 kb
37 of which 57 (3.9%) were characterized as viral using virSorter and virFinder (see methods).
38 Additionally, a cross-assembly of the metatranscriptomic viral contigs with metagenomes of the
39 same samples (N=12) yielded 9 more contigs (mean length 26,563 bp) characterized as viral.
40 Most of the contigs represent dsDNA viruses (N= 65) as apparent from their presence in
41 metagenomes, but one appears to be an RNA virus possibly infecting a eukaryotic host. This
42 contig contained an RNA-dependent-RNA-polymerase whose nearest match in NCBI non-
43 redundant database was marine Antarctic phytoplankton RNA virus PAL_E4⁹. These 66 viral
44 contigs revealed varied patterns of presence (in metagenomes) and activity (in
45 metatranscriptomes) in the three sites over a year (fig. 1).

46 Active non-synchronized viral infection would manifest as recruitment to an entire contig in both
47 metagenome and metatranscriptomes of the same sample. We found that patterns of mean
48 coverage from metagenomes and metatranscriptomes of our assembled viral contigs usually
49 differed, not just between metagenomes and metatranscriptomes but also between dates and
50 locations, implying widespread boom-bust dynamics of infection. While some variation may be
51 due to synchronization known for some photosynthetic and heterotrophic bacteria in the
52 ocean^{10,11} and for some of their phages¹², this explanation is less likely as samples were collected
53 from all sites within the same 4 hours morning-time window.
54 Some regional patterns were evident, e.g. some viral contigs were unique to the Port of LA (fig.
55 1), and that site always clustered separately from SPOT and CAT by Bray-Curtis similarity of
56 expression of viral contigs (sup. fig. 1B). This pattern corresponds to the difference in biotic
57 parameters between the port and the other sites (sup. fig. 2), though the port did not cluster
58 separately in microbial community composition by 16S-rRNA (sup. fig. 1A). The latter may
59 reflect offshore microbes brought in with the tide but less active than port organisms. Clustering
60 by metagenomic recruitment to viral contigs did not reveal consistent patterns by site or date
61 (sup. fig. 1C).
62



63
64
65
66
67
68
69
70
71
72

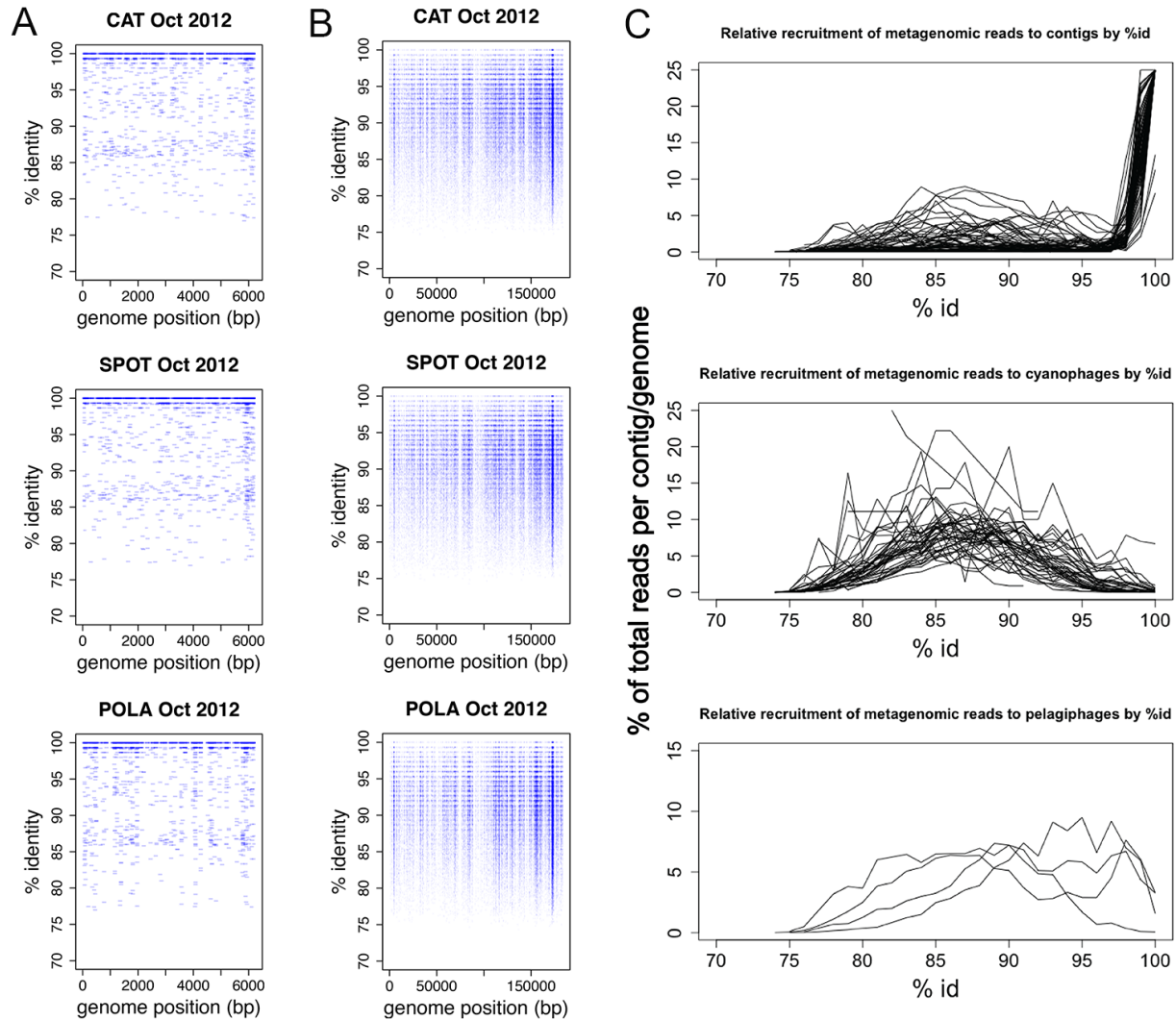
Figure 1: Mean coverage of 66 viral contigs across three sites (Port of LA – POLA, San Pedro Ocean Time-series – SPOT and Two harbors – CAT) and four dates (July 2012, October 2012, January 2013 and April 2013) in metagenomes (MG) and metatranscriptomes (MT). The bar heights are normalized to the highest mean coverage within the sample. Each cell in the color bar on the bottom represents a contig and corresponds with the column above it in all samples. Mean coverage was calculated excluding contig positions in the 4th quartile of coverage depth which can be biased by recruitment localized to a small portion of the contig (sup. fig. 3).

73 Ephemeral infections dominated the assembled landscape, as 56 out of 66 of the contigs only
74 appeared in few metatranscriptomes, presumably reflecting sporadic infections. Persistent
75 infections (mean coverage $\geq 0.75x$ in at least 3 out of 4 samples per site, 10 out of 66) were
76 limited to CAT and SPOT except for one that was persistent in all three sites. Moniruzzaman et
77 al.¹³ also recently demonstrated dominance of ephemeral dynamics in infections of marine
78 single-cell eukaryotes during an algal bloom. Bray-Curtis dissimilarity of the viral contigs within
79 each site was 80-100%, whereas the dissimilarity of microbial communities within site was
80 distributed around 50-70%. High dissimilarity indicates that even within site different viruses are
81 actively infecting in different seasons (sup. fig. 1D+E).

82 Moreover, assembled viral contigs appeared to be biased towards low-microdiversity (i.e. more
83 clonal) viruses. High diversity, extremely common in marine microorganisms¹⁴, tends to break
84 assemblies created with either read-overlaps or DeBruijn graphs^{15,16}. We expect that low virus
85 diversity could result from boom-bust lifestyle due to bottlenecks during “bursts”. This might
86 lead to a method bias towards ephemerally infecting viruses. Indeed, all the viral contigs we
87 assembled in this study appear to have many nearly identical relatives but few moderately close
88 ones as shown by recruitment plots (most recruitment at 98-100% identity and little recruitment
89 at 90-97%, fig. 2C), while some of the published pelagiphages had recruitment along most of the
90 genome and high mean coverage at up to 100% identity and yet did not assemble (fig. 2C, sup.
91 table 1).

92 The recruitment plots also reveal a common pattern of recruitment to short fragments near 100%
93 identity whereas the rest of the genome or contig is only recruited to at lower percentage if at all
94 (sup. fig. 3). This pattern highlights two issues: (1) some genes are so conserved or so often
95 laterally transferred that their partial sequences cannot be used to identify which phage is present
96 and (2) that mean coverage of contigs could be highly biased by these conserved regions which
97 needs to be considered when evaluating abundance of the contigs and for coverage-based
98 binning of genomes.

99 A previous report indicated that *Synechococcus* phage genomes occur in discrete “clouds” with a
100 discontinuity in recruitment below $\sim 95\%$ identity¹⁷. While this pattern exists for some
101 cyanophage genomes, and we often saw some gaps in coverage at $\sim 90-95\%$ consistent with that
102 idea (sup. fig. 3), it is by no means the rule in our data, especially for pelagiphages (fig. 2C). We
103 also note that widely used recruitment algorithms only map reads with a local or end-to-end
104 match at a very high percent identity, and would therefore miss much genetic diversity that may
105 be relevant (fig. 2B).



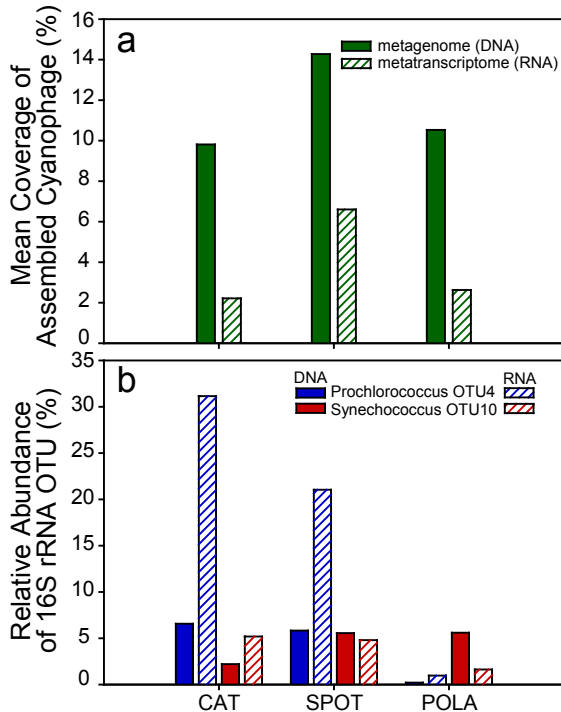
106
107

108 **Figure 2:** Metagenomic read recruitment to (A) an assembled cyanophage contig and (B)
109 *Prochlorococcus* phage P-HM2 genome. Most recruitment to the assembled contig is at 99-
110 100% identity (high density near 100% is not fully evident from the graph due to overlaps, see
111 C), whereas P-HM2 reveals a genomic continuum. (C) Recruitment as a function of percent ID
112 of reads demonstrates that assembled contigs mostly recruit at 100% ID and have few
113 moderately close relatives (top) whereas published genomes of cyanophages reveal clouds of
114 moderately close relatives but few matches near 100% (middle), and pelagiphages range from
115 100% down (bottom).

116

117 We were surprised not to find multiple cyanophage (especially myovirus) contigs, because such
118 cyanophages belong to the family *Myoviridae*, some of the most common dsDNA viruses in the
119 ocean¹⁸ and we know this region has a diverse community of myoviruses and cyanobacteria^{7,14}.
120 Few of the assembled viral contigs contained myoviral marker genes (e.g. capsid protein gp23)
121 (sup. Table 2). The only assembled contig that is with high certainty from a cyanophage is a
122 putative podovirus (see below). Recruitment of reads to published cyanophage genomes revealed
123 the likely reason for so few such contigs: high genomic diversity (fig. 2B) which probably broke

124 assemblies of T4-like cyanophages. We lacked assemblies despite persistent myovirus activity.
125 We assigned translated reads identified by a Gp23-HMM (Hidden Markov Model) to published
126 and assembled Gp23 proteins. Most versions of this marker gene from published genomes as
127 well as the nine assembled Gp23 ORFs were expressed persistently throughout all sites and dates
128 (sup. fig. 4). While the exact published genomes themselves were not present in our samples (fig.
129 2B), we posit that other T4-like cyanophages closely-related to those published are present and
130 persistently infecting their hosts.
131 Matching viral contigs and hosts is challenging, but we were able to use physiological
132 information and distributions among samples to make a likely match. Many cyanophages contain
133 a variety of genes that maintain photosynthetic activity in the host during infection, from “spare
134 parts” for photosynthetic reaction centers through regulation and optimization of those apparatus¹⁹.
135 In particular, viruses were shown to maintain photosystem II function during infection in order to
136 supply energy to the host, as transcription of host genes is shut down during infection and PS-II
137 proteins have a short lifetime^{20,21}. Our assembled cyanophage contig contained genes coding for
138 photosystem-II protein D1 (*psbA*) and high-light induced protein (*hli*) reportedly widespread in
139 cyanophages⁸. The putative cyanophage from which this contig was derived was actively
140 transcribed (presumably infecting its host) in all three sites only in October 2012 (fig. 4A). The
141 cyanobacterial community by 16S-rRNA was dominated in October by two operational
142 taxonomic units (OTUs): one *Synechococcus* and one *Prochlorococcus*. Both OTUs were present
143 at SPOT and CAT in October, but only *Synechococcus* was also present at POLA (fig. 4B).
144 Thus, we propose that this assembled contig is from a phage that infects *Synechococcus* OTU 10
145 which [has a 16S sequence over the amplified region](#) 100% identical to *Synechococcus* CC9902
146 of clade IV. On a phylogenetic tree of PS-II D1, translated PS-II D1 of this phage clustered
147 closely with a different phage isolated on *Synechococcus* (sup. fig. 5).
148
149
150



151
152

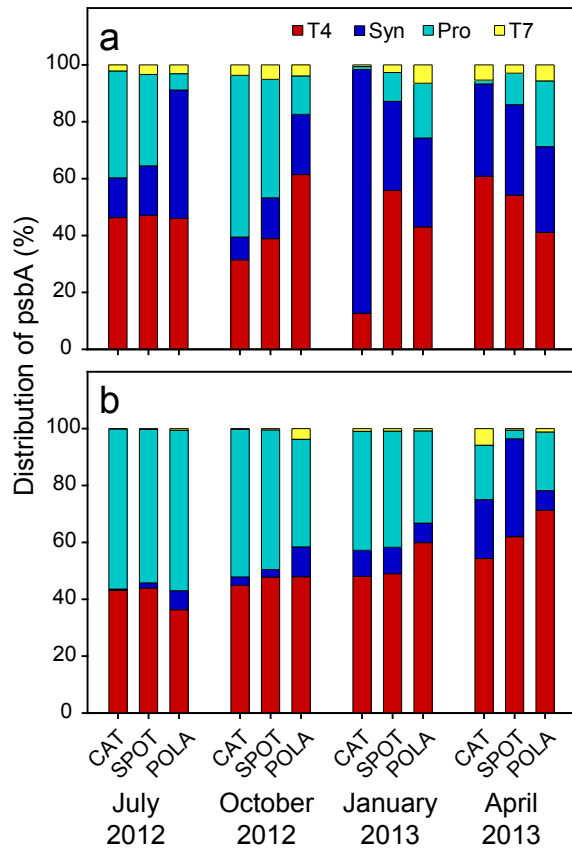
153 **Figure 3:** Presence and activity of the assembled cyanophage and its potential hosts in October
154 2012: (A) Mean coverage (quartiles 1-3) of assembled cyanophage (B) OTU relative abundance
155 by 16S-rRNA of the two most abundant cyanobacteria OTUs in order: *Prochlorococcus* in DNA,
156 *Prochlorococcus* in RNA, *Synechococcus* in DNA, *Synechococcus* in RNA. Note the near-
157 absence of *Prochlorococcus* in POLA, in contrast to *Synechococcus* and the phage, leading us to
158 infer the phage infects *Synechococcus*.

159

160 Because viruses and hosts both code for photosynthetic functions, a comparison of viral and
161 host-coded contributions to activity is possible. Sharon et al.²² previously showed viral *psbA*
162 gene can outnumber cyanobacterial *psbA* genes in metagenomes from the Mediterranean, and
163 showed viral gene expression is evident. We extended this to quantitatively partition gene
164 expression into bacterial contribution from *Synechococcus* and *Prochlorococcus* and viral
165 contribution from cyanomyoviruses and cyanopodoviruses, as evident from HMM-placed
166 translated reads onto our PS-II D1 phylogenetic tree. We found *psbA* transcripts of T4-like
167 cyanomyovirus origin generally accounted for roughly 50% of cyanobacterial and cyanophage
168 *psbA* transcripts. *Prochlorococcus* transcripts were almost always comparable to the T4-like
169 contribution. On several occasions, the viral version exceeded the cyanobacterial version in read
170 count (fig. 4).

171 We can roughly estimate the proportion of infected cyanobacteria from our *psbA* data and
172 compare it to previously published estimates. For cyanobacteria in marine systems, the highest
173 estimates of infection are roughly 50-60% infected at any given time^{2,17,23,24}. One consideration
174 when calculating the proportion of infected cyanobacteria is that during host infection, the
175 number of phage mRNA of *psbA* increases quickly during early infection until it becomes the
176 exclusive source of *psbA* transcripts in the cell^{20,21}. Another consideration is that, regardless their
177 source, host or virus, the abundance of *psbA* transcripts is comparable in infected and uninfected

178 cells²³. What we observe in the sample is a comparable contribution of T4-like phages and
179 cyanobacteria (fig. 5 D) at a ratio of 1.2 ± 0.6 (mean \pm standard deviation) phage/cyanobacteria,
180 which suggests that on average about half of the cyanobacteria are infected. This is in accordance
181 with the high end of published estimates, confirming that infection is an important part of
182 cyanobacterial ecology.
183



184
185

186 **Figure 4:** Distribution of psbA of T4-like phages, *Synechococcus*, *Prochlororoccus*, and T7-like
187 phages in (A) metagenomes and (B) metatranscriptomes.
188

189 In both metagenomes and metatranscriptomes, there is minor consistent recruitment to T7-like
190 cyanopodovirus psbA. However, in every sample the contribution of T7-like cyanopodoviruses
191 was very low compared to that of T4-like cyanomyoviruses. This could be due to the more
192 specific host range reported for cyanopodoviruses compared to cyanomyoviruses²⁵⁻²⁷. As T4-like
193 and T7-like cyanophages are reported to be strictly lytic²⁸, their presence in metagenomes results
194 from late infection genomic copies or virions within host cells, pseudolysogeny or phages that
195 adsorbed to cells or particles.

196 Extending metatranscriptomics methods as recently applied to marine eukaryotic viral
197 infection^{13,29,30}, we show the power of multiple approaches to track viral infection and dynamics
198 within the broad picoplankton community, using metatranscriptomes of the cellular fraction,
199 with particular examples in the cyanobacteria. Use of marker genes is especially important to
200 study viruses with many close relatives in the same environment (whose contigs assemble
201 poorly), whereas assemblies are useful for tracking ephemeral, more clonal viruses. The

202 observed infection dynamics can sometimes be used in combination with microbial community
203 structure and viral marker genes found within contigs to deduce a host. Use of metagenomes and
204 metatranscriptomes provides an insight into quantifiable viral contribution to photosynthesis and
205 to estimating the fraction of infected cyanobacteria.

206
207

208 **Methods**

209 *Sample collection*

210 Surface seawater was collected by bucket on 7/15/2012, 10/19/2012, 1/9/2013 and 4/24/2013 in
211 three locations: The Port of Los Angeles (33°42.75'N 118°15.55'W), the San Pedro Ocean Time-
212 series (33°33.00'N 118°24.01'W) and Two Harbors, Santa Catalina Island (33°27.18'N
213 118°28.51'W). Duplicate samples of 20 liters were filtered in each location through an 80 µm
214 mesh followed by a glass fiber syringe prefilter (Gelman, 4523) which collected the >1 µm size
215 fraction and a 0.2 µm PES Sterivex filter (Millipore, SVGPB1010) which collected the free-
216 living size fraction. RNAlater (Thermo-Fisher, AM7020) was added to each filter and filters
217 were flash frozen no more than 5 minutes post-filtration.

218 *Library preparation*

219 DNA and RNA were extracted simultaneously from Sterivex filters by bead-beating followed by
220 an AllPrep kit (Qiagen, 80204). An internal standard (ERCC RNA Spike-In Mix, Thermo-Fisher
221 4456740) was added into the lysate after bead-beating for quality assurance. RNA was enriched
222 for mRNA with RiboZero (Illumina, MRZB12424). Resulting mRNA was reverse transcribed
223 using SuperScript-III (Invitrogen, 18080-051). DNA and cDNA were sheared with Covaris m2
224 and size-selected for products larger than 300 bp. RNA libraries were prepared and barcoded
225 using NEBNext Ultra Directional RNA library Prep Kit for Illumina (E74205). DNA libraries
226 were prepared and barcoded with Ovation UltraLow Library Prep V2 (Nugen, 0344).
227 Metagenomes were sequenced on Illumina HiSeq 2x125 bp or 2x150 bp. Metatranscriptomes
228 were sequenced on Illumina HiSeq 2x250 bp.

229 *Read processing and assembly*

230 Raw metagenomics and metatranscriptomics reads were quality trimmed and filtered with
231 Trimmomatic version 0.33 with parameters LEADING:20 TRAILING:20
232 SLIDINGWINDOW:15:25³¹. Metatranscriptomic reads were merged with PEAR³², using the
233 default settings and residual ribosomal reads as well as the internal standard were removed
234 informatically. Merged reads from each sample separately were assembled with Megahit.
235 Contigs smaller than 2kbp from all samples were co-assembled with Newbler³³ version 2.9
236 (Roche) (minimum overlap 40bp minimum id 99%) and contigs larger than 2kbp from all
237 samples were co-assembled with minimus2³⁴ (minimum overlap 40bp minimum id 99%). Only
238 contigs larger than 5 Kbp were further analyzed.

239 *Identification and annotation of viral contigs*

240 Viral contigs were identified by VirSorter³⁵ using RefSeq on the CyVerse platform and only
241 contigs classified as category 1 or category 2 were considered. In addition, the contigs were
242 ranked using VirFinder³⁶ (rank >=0.95). Prodigal³⁷ was used to predict ORFs in those contigs,
243 and the amino acid sequences were searched against the nr database (August 12th 2016) using
244 blastp³⁸ and a maximum E-value 10⁻⁵. The annotations were used to verify viral contigs from the
245 VirFinder results. Contigs were verified to be non-chimeric by even recruitment.

246 Quality filtered metagenomic and metatranscriptomic reads were mapped back to these contigs
247 with Bowtie2 version 2.2.6 using the default settings and the expression patterns were identified
248 and visualized with Anvi'o³⁹ version 2.1.0.

249 *Microbial community composition analysis*

250 The V4-V5 regions of the 16S-rRNA coding gene were amplified from DNA and cDNA from all
251 samples using the 515-N-F and 926-R primers, and sequenced on an Illumina MiSeq 2x300 bp
252 (UC Davis genome center) along with a mock community as described in Parada et al.⁴⁰.

253 The ends of resulting reads were trimmed with PRINSEQ⁴¹ to a quality score higher than 20. The
254 trimmed reads were merged with USEARCH⁴² allowing for 3 mismatches in the overlap region.

255 Retained assembled reads were clustered with mothur⁴³ version 1.38.0 according to the MiSeq
256 and classified with SILVA version 119. Bray-Curtis dissimilarity and dendrograms were

257 calculated and plotted with R package vegan⁴⁴.

258 *Analysis of PS-II D1 protein sequences*

259 A curated set of PS-II D1 amino acid sequences of myoviruses, podoviruses, cyanobacteria and
260 eukaryotes (chloroplast) from Pfam⁴⁵ and RefSeq release 80 was downloaded. All sequences of

261 marine viral PS-II D1 were retained in addition to sequences of bacterial and eukaryotic taxa that
262 were identified in the 16S-rRNA community composition. One of the assembled contigs

263 contained a psbA gene coding for PS-II D1. The translated amino acid sequences were added to
264 the set of proteins.

265 Merged reads from the metatranscriptomes and unmerged forward reads from the metagenomes
266 were aligned with blastx³⁸ against this set demanding an e-value of 10^{-5} . The reads that passed

267 the filter were translated using bioPython⁴⁶ into amino acids according to the reading frame
268 indicated by the blastx start and end values.

269 Following the protocol used in Ignacio-Espinoza et al.⁴⁷ total of 158 sequences were aligned with
270 mafft⁴⁸ version 7.305b with parameters set to globalpair, gap open penalty 1.5, gap extension

271 penalty 0.5 and scoring matrix BLOSUM30. Informative blocks were identified using Gblocks⁴⁹
272 version 0.91b with a minimum block length 5, blocks represent at least half of the sequences and

273 allowing gaps (b3=50, b4=5, b5=h). The blocks were used to build a maximum likelihood
274 phylogenetic tree using RAxML⁵⁰ (best of 20 trees, gamma model and WAG substitution

275 matrix). A hidden Markov Model (HMM) of the same set was also built with hmmer 3.0⁵¹. The
276 translated metagenomics and metatranscriptomics amino acid sequences were searched using the

277 HMM and a threshold of e-value 10^{-5} . A total of 190,928 translated metatranscriptomics reads
278 and 72,292 metagenomics reads from all samples remained after this step. Those reads were

279 locally aligned to the HMM using hmmer 3.0 function hmmalign and placed into the
280 phylogenetic tree using pplacer⁵² version v1.1.alpha17 (sup. fig. 6).

281 *Analysis of gp23 protein sequences*

282 Metatranscriptomic and metagenomics reads were searched against a set of T4-like clusters of
283 orthologous groups (COGs) with an E-value threshold of 10^{-5} . 89,768 metatranscriptomic reads

284 and 134,995 metagenomic reads were annotated as gp23. An HMM of gp23 was built as
285 described previously and translated reads were searched and placed with pplacer. The tree was

286 visualized by the Interactive Tree Of Life (iTOL)⁵³.

287 *Recruitment to phage genomes*

288 The four currently available full pelagiphage genomes were downloaded from NCBI and
289 concatenated with assembled viral contigs from metatranscriptomes the metagenomes as well as

290 with published cyanophage genomes downloaded from NCBI RefSeq. Metagenomic and
291 metatranscriptomics reads were searched against the genomes dataset with blastn default

292 settings. For metagenomes only hits longer than 100bp were retained, and for
293 metatranscriptomes only hits longer than 200bp. Hits were then plotted against the genomes
294 using R⁵⁴.

295 *Data availability*

296 All data can be found on EMBL-ENA under project number PRJEB12234. Raw
297 metatranscriptomics sequences accession numbers are ERS1864892-ERS1864903, and negative
298 control library sequences accession number is ERR2089009. Raw metagenomic sequences
299 accession numbers are ERS1869885-ERS1869896 and negative control accession number is
300 ERS1872073. Assembled viral contigs accession numbers are ERZ474118-ERZ474183.

301

302 **Acknowledgements**

303 The authors would like to thank R. Sachdeva, N. Ahlgren, A. Parada, L. Berdjeb, E. Graham, M.
304 Lee, J. Ren, F. Sun and T. Delmont for insightful discussions and advice on bioinformatics
305 analyses. We thank Catherine Roney-Garcia, the Sundiver crew and the USC Wrigley Institute
306 of Environmental Studies for logistic support. This work was supported by NSF grant 1136818,
307 Gordon and Betty Moore Foundation Marine Microbiology Initiative grant GBMF3779 and
308 Norma and Jerol Sonosky summer fellowship to E.T.S.

309

310 **References:**

- 311 1. Proctor, L. M., & Fuhrman, J. A. (1990). Viral mortality of marine bacteria and
312 cyanobacteria. *Nature*, 343(6253), 60.
- 313 2. Suttle, C. A. (2007). Marine viruses--major players in the global ecosystem. *Nature*
314 *reviews. Microbiology*, 5(10), 801.
- 315 3. Lima-Mendez, G., Faust, K., Henry, N., Decelle, J., Colin, S., Carcillo, F., ... & Bittner,
316 L. (2015). Determinants of community structure in the global plankton
317 interactome. *Science*, 348(6237), 1262073.
- 318 4. Brum, J. R., Ignacio-Espinoza, J. C., Roux, S., Doulcier, G., Acinas, S. G., Alberti, A., ...
319 & Gorsky, G. (2015). Patterns and ecological drivers of ocean viral
320 communities. *Science*, 348(6237), 1261498.
- 321 5. Paez-Espino, D., Eloie-Fadrosh, E. A., Pavlopoulos, G. A., Thomas, A. D., Huntemann,
322 M., Mikhailova, N., ... & Kyrpides, N. C. (2016). Uncovering Earth's
323 virome. *Nature*, 536(7617).
- 324 6. Nishimura, Y., Watai, H., Honda, T., Mihara, T., Omae, K., Roux, S., ... & Sullivan, M.
325 B. (2017). Environmental viral genomes shed new light on virus-host interactions in the
326 ocean. *mSphere*, 2(2), e00359-16.
- 327 7. Chow, C. E. T., & Fuhrman, J. A. (2012). Seasonality and monthly dynamics of marine
328 myovirus communities. *Environmental microbiology*, 14(8), 2171-2183.
- 329 8. Adriaenssens, E. M., & Cowan, D. A. (2014). Using signature genes as tools to assess
330 environmental viral ecology and diversity. *Applied and environmental*
331 *microbiology*, 80(15), 4470-4480.
- 332 9. Miranda, J. A., Culley, A. I., Schvarcz, C. R., & Steward, G. F. (2016). RNA viruses as
333 major contributors to Antarctic viroplankton. *Environmental microbiology*, 18(11),
334 3714-3727.
- 335 10. Ottesen, E. A., Young, C. R., Eppley, J. M., Ryan, J. P., Chavez, F. P., Scholin, C. A., &
336 DeLong, E. F. (2013). Pattern and synchrony of gene expression among sympatric marine

- 337 microbial populations. *Proceedings of the National Academy of Sciences*, 110(6), E488-
338 E497.
- 339 11. Ottesen, E. A., Young, C. R., Gifford, S. M., Eppley, J. M., Marin, R., Schuster, S. C., ...
340 & DeLong, E. F. (2014). Multispecies diel transcriptional oscillations in open ocean
341 heterotrophic bacterial assemblages. *Science*, 345(6193), 207-212.
- 342 12. Jia, Y., Shan, J., Millard, A., Clokie, M. R., & Mann, N. H. (2010). Light-dependent
343 adsorption of photosynthetic cyanophages to *Synechococcus* sp. WH7803. *FEMS*
344 *microbiology letters*, 310(2), 120-126.
- 345 13. Moniruzzaman, M., Wurch, L. L., Alexander, H., Dyhrman, S. T., Gobler, C. J., &
346 Wilhelm, S. W. (2017). Virus-host relationships of marine single-celled eukaryotes
347 resolved from metatranscriptomics. *Nature Communications*, 8.
- 348 14. Needham, D. M., Sachdeva, R., & Fuhrman, J. A. (2017). Ecological dynamics and co-
349 occurrence among marine phytoplankton, bacteria and myoviruses shows microdiversity
350 matters. *The ISME Journal*.
- 351 15. Awad, S., Irber, L., & Brown, C. T. (2017). Evaluating Metagenome Assembly on a
352 Simple Defined Community with Many Strain Variants. *bioRxiv*, 155358.
- 353 16. Martinez-Hernandez, F., Fornas, O., Gomez, M. L., Bolduc, B., de la Cruz Pena, M. J.,
354 Martínez, J. M., ... & Sullivan, M. B. (2017). Single-virus genomics reveals hidden
355 cosmopolitan and abundant viruses. *Nature Communications*, 8.
- 356 17. Deng, L., Ignacio-Espinoza, J. C., Gregory, A. C., Poulos, B. T., Weitz, J. S.,
357 Hugenholtz, P., & Sullivan, M. B. (2014). Viral tagging reveals discrete populations in
358 *Synechococcus* viral genome sequence space. *Nature*, 513(7517), 242.
- 359 18. Williamson, S. J., Allen, L. Z., Lorenzi, H. A., Fadrosch, D. W., Bрами, D., Thiagarajan,
360 M., ... & Venter, J. C. (2012). Metagenomic exploration of viruses throughout the Indian
361 Ocean. *PLoS One*, 7(10), e42047.
- 362 19. Hurwitz, B. L., & U'Ren, J. M. (2016). Viral metabolic reprogramming in marine
363 ecosystems. *Current opinion in microbiology*, 31, 161-168.
- 364 20. Lindell, D., Jaffe, J. D., Johnson, Z. I., Church, G. M., & Chisholm, S. W. (2005).
365 Photosynthesis genes in marine viruses yield proteins during host
366 infection. *Nature*, 438(7064), 86.
- 367 21. Clokie, M. R., Shan, J., Bailey, S., Jia, Y., Krisch, H. M., West, S., & Mann, N. H.
368 (2006). Transcription of a 'photosynthetic' T4-type phage during infection of a marine
369 cyanobacterium. *Environmental Microbiology*, 8(5), 827-835.
- 370 22. Sharon, I., Tzahor, S., Williamson, S., Shmoish, M., Man-Aharonovich, D., Rusch, D. B.,
371 ... & Adir, N. (2007). Viral photosynthetic reaction center genes and transcripts in the
372 marine environment. *The ISME journal*, 1(6), 492.
- 373 23. Proctor, L. M., & Fuhrman, J. A. (1990). Viral mortality of marine bacteria and
374 cyanobacteria. *Nature*, 343(6253), 60.
- 375 24. Wommack, K. E., & Colwell, R. R. (2000). Virioplankton: viruses in aquatic
376 ecosystems. *Microbiology and molecular biology reviews*, 64(1), 69-114.
- 377 25. Sullivan, M. B., Waterbury, J. B., & Chisholm, S. W. (2003). Cyanophages infecting the
378 oceanic cyanobacterium *Prochlorococcus*. *Nature*, 424(6952), 1047.
- 379 26. Millard, A. D., & Mann, N. H. (2006). A temporal and spatial investigation of
380 cyanophage abundance in the Gulf of Aqaba, Red Sea. *Journal of the Marine Biological*
381 *Association of the United Kingdom*, 86(3), 507-515.

- 382 27. Wang, K., & Chen, F. (2008). Prevalence of highly host-specific cyanophages in the
383 estuarine environment. *Environmental microbiology*, *10*(2), 300-312.
- 384 28. Martin, E., & Benson, R. (1988). Phages of cyanobacteria. *The bacteriophages*, *2*, 607-
385 645.
- 386 29. Dupont, C. L., McCrow, J. P., Valas, R., Moustafa, A., Walworth, N., Goodenough, U.,
387 ... & Mann, E. (2015). Genomes and gene expression across light and productivity
388 gradients in eastern subtropical Pacific microbial communities. *The ISME journal*, *9*(5),
389 1076.
- 390 30. Allen, L. Z., McCrow, J. P., Ininbergs, K., Dupont, C. L., Badger, J. H., Hoffman, J. M.,
391 ... & Venter, J. C. (2017). The Baltic Sea Virome: Diversity and Transcriptional Activity
392 of DNA and RNA Viruses. *mSystems*, *2*(1), e00125-16.
- 393 31. Bolger, A. M., Lohse, M., & Usadel, B. (2014). Trimmomatic: a flexible trimmer for
394 Illumina sequence data. *Bioinformatics*, *30*(15), 2114-2120.
- 395 32. Zhang, J., Kobert, K., Flouri, T., & Stamatakis, A. (2013). PEAR: a fast and accurate
396 Illumina Paired-End reAd mergeR. *Bioinformatics*, *30*(5), 614-620.
- 397 33. Margulies, M., Egholm, M., Altman, W. E., Attiya, S., Bader, J. S., Bemben, L. A., ... &
398 Dewell, S. B. (2005). Genome sequencing in open microfabricated high density picoliter
399 reactors. *Nature*, *437*(7057), 376.
- 400 34. Sommer, D. D., Delcher, A. L., Salzberg, S. L., & Pop, M. (2007). Minimus: a fast,
401 lightweight genome assembler. *BMC bioinformatics*, *8*(1), 64.
- 402 35. Roux, S., Enault, F., Hurwitz, B. L., & Sullivan, M. B. (2015). VirSorter: mining viral
403 signal from microbial genomic data. *PeerJ*, *3*, e985.
- 404 36. Ren, J., Ahlgren, N. A., Lu, Y. Y., Fuhrman, J. A., & Sun, F. (2017). VirFinder: a novel
405 k-mer based tool for identifying viral sequences from assembled metagenomic
406 data. *Microbiome*, *5*(1), 69.
- 407 37. Hyatt, D., Chen, G. L., LoCascio, P. F., Land, M. L., Larimer, F. W., & Hauser, L. J.
408 (2010). Prodigal: prokaryotic gene recognition and translation initiation site
409 identification. *BMC bioinformatics*, *11*(1), 119.
- 410 38. Camacho, C., Coulouris, G., Avagyan, V., Ma, N., Papadopoulos, J., Bealer, K., &
411 Madden, T. L. (2009). BLAST+: architecture and applications. *BMC*
412 *bioinformatics*, *10*(1), 421.
- 413 39. Eren, A. M., Esen, Ö. C., Quince, C., Vineis, J. H., Morrison, H. G., Sogin, M. L., &
414 Delmont, T. O. (2015). Anvi'o: an advanced analysis and visualization platform for
415 'omics data. *PeerJ*, *3*, e1319.
- 416 40. Parada, A. E., Needham, D. M., & Fuhrman, J. A. (2016). Every base matters: assessing
417 small subunit rRNA primers for marine microbiomes with mock communities, time series
418 and global field samples. *Environmental microbiology*, *18*(5), 1403-1414.
- 419 41. Schmieder, R., & Edwards, R. (2011). Quality control and preprocessing of metagenomic
420 datasets. *Bioinformatics*, *27*(6), 863-864.
- 421 42. Edgar, R. C. (2010). Search and clustering orders of magnitude faster than
422 BLAST. *Bioinformatics*, *26*(19), 2460-2461.
- 423 43. Schloss, P. D., Westcott, S. L., Ryabin, T., Hall, J. R., Hartmann, M., Hollister, E. B., ...
424 & Sahl, J. W. (2009). Introducing mothur: open-source, platform-independent,
425 community-supported software for describing and comparing microbial
426 communities. *Applied and environmental microbiology*, *75*(23), 7537-7541.

- 427 44. Oksanen, J., Kindt, R., Legendre, P., O'Hara, B., Stevens, M. H. H., Oksanen, M. J., &
428 Suggests, M. A. S. S. (2007). The vegan package. *Community ecology package*, 10, 631-
429 637. <http://vegan.r-forge.r-project.org>
- 430 45. Finn, R. D., Coggill, P., Eberhardt, R. Y., Eddy, S. R., Mistry, J., Mitchell, A. L., ... &
431 Salazar, G. A. (2016). The Pfam protein families database: towards a more sustainable
432 future. *Nucleic acids research*, 44(D1), D279-D285.
- 433 46. Cock, P. J., Antao, T., Chang, J. T., Chapman, B. A., Cox, C. J., Dalke, A., ... & De
434 Hoon, M. J. (2009). Biopython: freely available Python tools for computational
435 molecular biology and bioinformatics. *Bioinformatics*, 25(11), 1422-1423.
- 436 47. Ignacio-Espinoza, J. C., & Sullivan, M. B. (2012). Phylogenomics of T4 cyanophages:
437 lateral gene transfer in the 'core' and origins of host genes. *Environmental*
438 *microbiology*, 14(8), 2113-2126.
- 439 48. Katoh, K., & Standley, D. M. (2013). MAFFT multiple sequence alignment software
440 version 7: improvements in performance and usability. *Molecular biology and*
441 *evolution*, 30(4), 772-780.
- 442 49. Castresana, J. (2000). Selection of conserved blocks from multiple alignments for their
443 use in phylogenetic analysis. *Molecular biology and evolution*, 17(4), 540-552.
- 444 50. Stamatakis, A. (2014). RAxML version 8: a tool for phylogenetic analysis and post-
445 analysis of large phylogenies. *Bioinformatics*, 30(9), 1312-1313.
- 446 51. Johnson, L. S., Eddy, S. R., & Portugaly, E. (2010). Hidden Markov model speed
447 heuristic and iterative HMM search procedure. *BMC bioinformatics*, 11(1), 431.
- 448 52. Matsen, F. A., Kodner, R. B., & Armbrust, E. V. (2010). pplacer: linear time maximum-
449 likelihood and Bayesian phylogenetic placement of sequences onto a fixed reference
450 tree. *BMC bioinformatics*, 11(1), 538.
- 451 53. Letunic, I., & Bork, P. (2016). Interactive tree of life (iTOL) v3: an online tool for the
452 display and annotation of phylogenetic and other trees. *Nucleic acids research*, 44(W1),
453 W242-W245.
- 454 54. R Core Team (2016) <https://www.R-project.org/>